GA–A24353

OBSERVATION OF SELF-MITIGATION OF A DENSITY LIMIT DISRUPTION IN DIII–D

by
D.S. GRAY, E.M. HOLLMANN, D.G. WHYTE, A.Yu. PIGAROV,
S.I. KRASHENINNIKOV, J.A. BOEDO, and D.A. HUMPHREYS

AUGUST 2003

DISCLAIMER

GA–A24353

OBSERVATION OF SELF-MITIGATION OF A DENSITY LIMIT DISRUPTION IN DIII–D

by
D.S. GRAY,* E.M. HOLLMANN,* D.G. WHYTE,† A.Yu. PIGAROV,* S.I. KRASHENINNIKOV,* J.A. BOEDO,* and D.A. HUMPHREYS

This is a preprint of a paper to be presented at the 30th European Physical Society Conference on Controlled Fusion and Plasma Physics, St Petersburg, Russia, July 7–11, 2003 and to be published in the *Proceedings.*

*University of California, San Diego, California.
†University of Wisconsin, Madison, Wisconsin.

Work supported by
the U.S. Department of Energy
under Contract Nos. DE-FG03-95ER54294,
DE-FG02-89ER53297, and DE-AC03-99ER54463

GENERAL ATOMICS PROJECT 30033
AUGUST 2003

Observation of Self-Mitigation of a Density Limit Disruption in DIII-D

D.S. Gray[1], E.M. Hollmann[1], D. G. Whyte[2], A.Yu. Pigarov[1], S.I. Krasheninnikov[1],
J.A. Boedo[1], and D.A. Humphreys[3]

[1]*Center for Energy Research, University of California at San Diego, La Jolla, CA, 92093-0417 USA*
[2]*University of Wisconsin, Madison, WI, 53706 USA*
[3]*General Atomics, P.O. Box 83608, La Jolla, CA, 92186-5608 USA*

Density limit disruptions set an upper bound on the electron density in tokamaks and are important for future reactor-size tokamaks, which will typically need to operate at high densities to achieve ignition [1]. In the standard picture of disruptions [2], a large MHD mode, or combination of MHD modes, causes a mixing of previously nested magnetic flux surfaces across much of the profile. Rapid heat and particle transport across the separatrix result, and the thermal energy of the discharge is lost along open field lines into the divertor on a millisecond time scale or faster.

In this work, a density limit disruption is initiated by ramping up the density in a lower single-null discharge in the DIII-D tokamak [3]. As in most disruptions, a large MHD precursor is observed. However, in contrast with the disruption scenario described above, it is found that the plasma thermal energy, rather than being conducted into the divertor, is dominantly lost by radiation to the main chamber walls. This has been referred to as “self-mitigation” of the disruption, in comparison to the intentional mitigation of localized heat loads in disruptions by the introduction of pellets or liquid or gas jets to enhance radiation. The self-mitigation effect appears to result from a release of neutrals (deuterium and carbon) from the graphite vacuum vessel walls. These results could have favorable implications for the severity of divertor heat loads during density limit disruptions in future large tokamaks.

Figure 1 shows time traces from various diagnostics in the disruption studied here: (a) the amplitude of magnetic fluctuations (dominantly from an n=1 MHD mode), (b) a midplane soft x-ray view chord (showing the core electron temperature collapse), (c) a midplane XUV photodiode view chord (showing total radiated power [4]), (d) a midplane D_β filterscope view chord (indicating deuterium ionization), (e) the total electron number estimated from CO_2 interferometer signals (demonstrating neutral influx), and (f) the toroidal plasma current (showing the slow current quench). From the core electron temperature collapse, Fig. 1(b), it can be seen that the thermal quench of the plasma occurs around t = 1912 ms. The thermal quench coincides with significant MHD activity, Fig. 1(a); however, it is not clear from the timing of the traces if the MHD activity begins before or after the enhanced recycling seen in Fig. 1(d).

To estimate the spatial origin of the thermal quench radiation spike, a zonal analysis of XUV photodiode array data is performed. The XUV array viewing geometry is shown in Fig. 2. Thirty view chords intersect the plasma at a single toroidal location. The spectral sensitivity of the diodes is 1 eV to 5 keV, which covers the full range of electron temperatures (and emission energies) expected in DIII-D. The red lines indicate the zone boundaries. The plasma emission is assumed to be constant within each zone boundary, allowing inversion of the plasma emissivity from the line-integrated XUV brightnesses. The boundaries of zones are obtained using EFIT magnetic flux surfaces reconstructed immediately before the onset of the thermal quench. The zonal inversion of the xuv brightnesses shows that the radiation during the density limit disruption comes primarily from the main chamber, rather than the divertor. This can be seen in Fig. 3(a), where the plasma emissivity is separated into main chamber (sum of radiation from regions 1-5) and divertor (sum of regions 6-7) radiated power. The total energy radiated during the main radiation spike of Fig. 3(a) is calculated to be about 0.8 MJ, accounting completely for the estimated 0.6 MJ of initial plasma thermal energy. The dashed red line is the total divertor heat load obtained from IR thermography, showing reasonably good agreement with the XUV data.

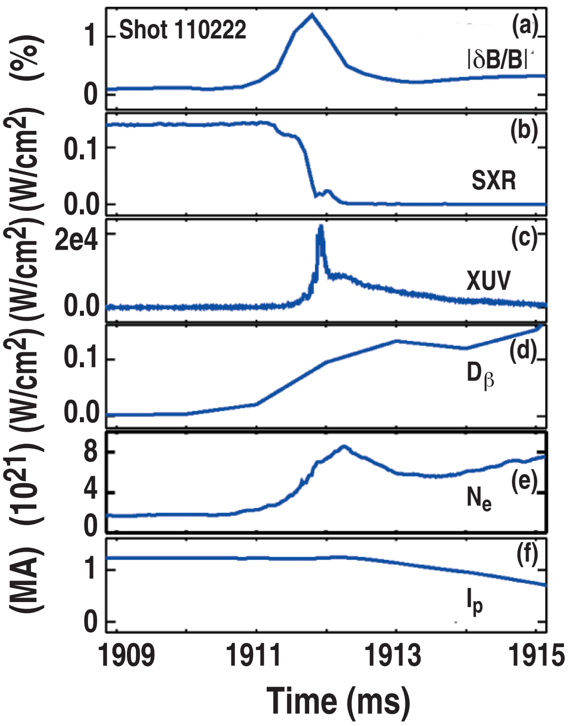

Fig. 1. Time traces from the density limit disruption.

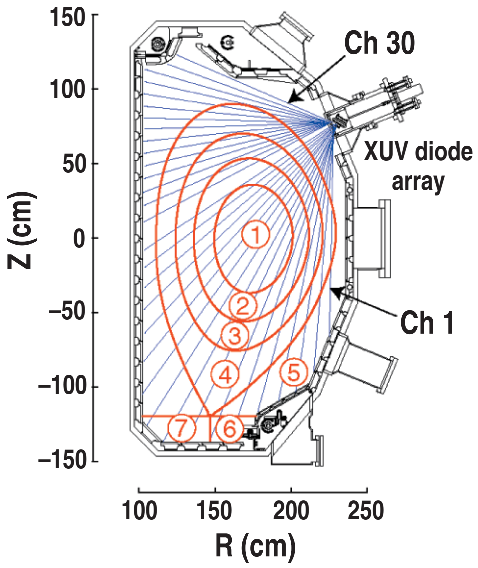

Fig. 2. DIII-D cross section showing XUV diode array view chord geometry and boundaries of emission zones used for inverting brightness signals.

For comparison with the density limit disruption, radiated power measurements are shown from a current limit disruption, Fig. 3(b), a downward VDE disruption, Fig. 3(c), and a downward VDE preemptively mitigated by a massive main chamber injection of neon gas, Fig. 3(d) [5]. In the current limit and unmitigated VDE disruptions, it can be seen that the dominant heat load is to the divertor, as expected (all these discharges are lower single-null diverted).

The large main chamber radiation seen in Fig. 3(a), together with the fourfold increase in electron number seen in Fig. 1(e), clearly demonstrates a large influx of neutral particles into the plasma during the density limit disruption. These neutrals are probably released dominantly from the main chamber walls, since neutrals emitted from the divertor are expected to ionize within a mean free path of about 10 cm and then get re-deposited as ions back into the divertor, thus not causing significant main chamber radiation.

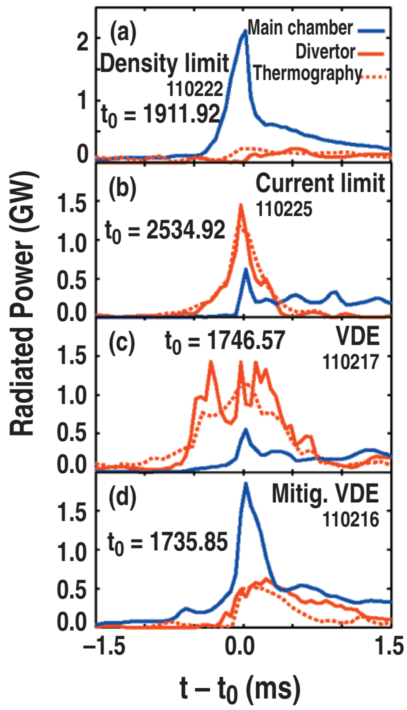

Fig. 3. Power radiated from the divertor and main chamber as function of time for four different types of disruptions. In each case, t_0 corresponds to the peak in total radiated power.

The composition of neutrals emitted from walls appears to consist dominantly of deuterium mixed with some (of order 5%) carbon. This can be seen from main chamber filterscope measurements of the D_β (4681 Å) over C_{III} (4650 Å) line ratio, which was found to be 1.1 before the disruption and 0.7 at the peak of the thermal quench. Using a sx/b (ionizations per photon) ratio of 140 for D_β and 7 for C_{III} [6], the measured line ratios give estimated carbon fractions of $f_c = 0.06$ before the disruption and $f_c = 0.04$ during the disruption. It is likely that the carbon neutrals, while the minority species, are the dominant source of radiated power during the thermal quench, since a typical D atom is expected to radiate only about 7 eV, on average, before becoming ionized [7], thus giving only 6 kJ of radiated energy from the $6{\times}10^{21}$ new electrons seen in Fig. 1(e).

The cause of the main chamber impurity release is not well-known at this point. Since most of the plasma thermal energy is radiated away, rather than conducted into the walls, it seems unlikely that the standard mechanisms of thermal desorption of deuterium and ion sputtering of carbon can be the dominant release mechanisms. It is possible that the observed neutral release is the result of a transient materials physics effect, *i.e.* a sudden release of deuterium and hydrocarbons from the highly saturated plasma-facing graphite tiles.

The transport mechanism by which the impurities are mixed into the core on the thermal quench time scale is also poorly understood at this point. Analysis of the XUV signal delays between different view chords indicates a large impurity diffusion coefficient of order $D_\perp \approx 100\ \mathrm{m}^2/\mathrm{s}$. This is much larger than the impurity transport rate $D_\perp \approx 1\ \mathrm{m}^2/\mathrm{s}$ observed previously during normal (H-mode) operation [8] but is roughly in agreement with impurity transport observed during disruptions triggered by impurity pellet injection [9]. It is thought that large-scale magnetic reconnection events could be responsible for transport rates of this magnitude [10].

This work was supported by the U.S. Department of Energy under Grants DE-FG03-95ER54294, DE-FG02-89ER53297, and Contract DE-AC03-99ER54463. The authors acknowledge assistance from the DIII-D and PISCES technical support staff, as well as help with data analysis from Drs. C.J. Lasnier, T.E. Evans, A.W. Leonard, E.J. Strait, and R.A. Moyer.

[1] ITER Physics Expert Groups, *Nucl. Fusion* **39**, 2577 (1999).

[2] *Tokamaks*, J. Wesson (Clarendon Press, Oxford, 1997).

[3] Luxon, J.L., *Nucl. Fusion* **42**, 614 (2002).

[4] Gray, D.S., Luckhardt, S.C., Kellman, A.G., *et al.*., "Time Resolved Radiated Power During Tokamak Disruptions and Spectal Averaging of AXUV Photodiode Response in DIII-D," submitted to *Rev. Sci. Inst.*

[5] Whyte, D.G., Jernigan, T.C., Humphreys, D.A., *et al.*., *Phys. Rev. Lett.* **89**, 055001 (2002).

[6] Summers, H.P., "Atomic Data and Analysis Structure: User's Manual," JET Joint Undertaking Report JET-IR94, 1994.

[7] Pigarov, A., and Krasheninnikov, *Phys. Lett. A* **222**, 251 (1999).

[8] Wade, M.R., Luce, T.C., and Petty, C.C., *Phys. Rev. Lett.* **79**, 419 (1997).

[9] Whyte, D.G., Evans, T.E., Hyatt, A.W., *et al.*, *Phys. Rev. Lett.* **81**, 4392 (1998).

[10] Kadomtzev, B.B., and Pogutse, D.P., *Sov. Phys. JETP* **38**, 283 (1974).